Bimolecular recombination and fill factor in crystalline polymer solar cells

AUTHOR(S):

Fukuhara, Tomohiro; Tamai, Yasunari; Osaka, Itaru; Ohkita, Hideo

CITATION:

Fukuhara, Tomohiro ...[et al]. Bimolecular recombination and fill factor in crystalline polymer solar cells. Japanese Journal of Applied Physics 2018, 57(853): 08RE01.

ISSUE DATE:

2018-08

URL:

http://hdl.handle.net/2433/232600

Bimolecular recombination and fill factor in crystalline polymer solar cells

Tomohiro Fukuhara[1], Yasunari Tamai[1], Itaru Osaka[2], and Hideo Ohkita[1*]

[1]*Department of Polymer Chemistry, Graduate School of Engineering, Kyoto University, Katsura, Kyoto 615-8510, Japan*

[2]*Department of Applied Chemistry, Graduate School of Engineering, Hiroshima University, 1-4-1 Kagamiyama, Higashi-Hiroshima, Hiroshima 739-8527, Japan*

[*]E-mail: ohkita@photo.polym.kyoto-u.ac.jp

Fill factor (FF) is one of the important photovoltaic parameters, which is limited mainly by charge recombination in solar cells. It is still a challenging issue to realize high FF with a thick active layer, which is required for the development of efficient bulk-heterojunction polymer solar cells. In this study, we discussed how recombination losses limit charge collection efficiency in polymer solar cells with low FF by measuring transient optoelectronic techniques. As a result, we found that geminate recombination is almost voltage-independent, that bimolecular recombination is suppressed significantly under open-circuit condition, and that hole and electron mobilities are low and imbalanced. We therefore concluded that the low collection efficiency is caused by bimolecular recombination of accumulated charges due to low and imbalanced mobilities.

1. Introduction

Bulk-heterojunction polymer solar cells have recently been attracting significant attention as renewable energy sources because of inexpensive production of lightweight and flexible devices. The power conversion efficiency (PCE) has been raised in the last decade over 10%[1–4] and now exceeded 13%[5]. For further improvement in photocurrent generation, thick active layers are needed to harvest many more photons from the solar light. In most cases, however, the active layer is typically as thin as ~100 nm[6–8] and thick active layers would degrade a fill factor (FF) because charge carriers have to diffuse long distance to electrodes and hence are likely to recombine bimolecularly. In other words, FF is mainly limited by charge recombination in competition with charge collection. Thus, of particular importance is to maintain high FF with a thick active layer, which is still one of challenging issues for highly efficient polymer solar cells. Recently, several polymer solar cells have been reported to exhibit high FF even with a thick active layer above 200 nm[9–13]. However, little is known about the origin of such high FF in polymer solar cells.

Previously, we studied recombination dynamics in highly efficient polymer solar cells based on naphtho[1,2-c:5,6-c']bis[1,2,5]thiadiazole (NTz)-based polymers (PNTz4TF*x*, *x* = 0 or 2) and a C_{70} fullerene derivative ($PC_{71}BM$)[4,12,13]. The NTz-based polymers are highly crystalline and hence exhibit high hole mobility. As a result, the optimum thickness was as thick as 270 nm for PNTz4T/$PC_{71}BM$ and 230 nm for PNTz4TF2/$PC_{71}BM$ solar cells. Interestingly, FF was still as high as >0.65 even for such thick devices. We found that bimolecular recombination is reduced significantly and thus charge carriers are efficiently collected to each electrode before they recombine bimolecularly even with a thick active layer[13]. These findings suggest that high FF with a thick active layer is due to high mobility and reduced recombination.

Herein, we have studied recombination dynamics in polymer solar cells based on poly[(4,4-bis(2-ethylhexyl)dithieno-[3,2-*b*:2',3'-*d*]silole)-2,6-diyl-*alt*-(2,1,3-benzothiadiazole)-4,7-diyl] (PSBTBT)[14–17] and $PC_{71}BM$. Similarly to NTz-based polymers, the PSBTBT is also a crystalline polymer. However, the optimum thickness was as thin as 100 nm[18] because FF was degraded with the increase in the active layer thickness. In order to address the origin of such low FF, we studied geminate and bimolecular recombination losses by measuring transient absorption, transient photovoltage and transient

photocurrent of PSBTBT/$PC_{71}BM$ solar cells.

2. Experimental methods

The photovoltaic devices were fabricated as follows. Indium–tin-oxide (ITO) substrates were cleaned by ultrasonication in toluene, acetone, and ethanol each for 15 min, dried with N_2 gas flow, and treated with a UV–ozone cleaner for 30 min. A transparent conductive layer of poly(3,4-ethylenedioxythiophene):poly(4-styrenesulfonate) (PEDOT:PSS; H. C. Starck, PH500) was spin-coated on the ITO substrate, which was subsequently annealed at 140 °C for 10 min in air. A photoactive layer was spincoated from a 1,2-dichlorobenzene solution of PSBTBT (1-Material) and $PC_{71}BM$ (Frontier Carbon, E110) (1 : 1.5 by weight). Finally, a metal electrode of Ca (3 nm)/Al (80 nm) was thermally deposited on top of the active layer under vacuum at 4×10^{-4} Pa.

For the solar cells fabricated, transient photovoltage (TPV) and transient photocurrent (TPC) measurements were performed under bias white light illumination from a 500-W Xenon lamp (Tonika, XEF-152S) with various intensities from ~0.1 to 1 sun. A small perturbation pump pulse at 500 nm was provided from a dye laser (Photon Technology International, GL-301) that was pumped with a nitrogen laser (Photon Technology International, GL-3300). The transient voltage generated by the laser pulse was monitored with a 500-MHz digital oscilloscope (Tektronix, TDS3052B). For TPV measurements, the input impedance of the oscilloscope was set to 1 MΩ to hold the device at open-circuit. For TPC measurements, the transient voltage was measured through a 50 Ω resistor.

Electric field-dependent transient absorption were measured for the devices fabricated as follows. As mentioned above, ITO substrates were cleaned by the same method. A polyvinyl alcohol (PVA) film of 50 nm was spincoated from a water solution on top of that as an insulating layer. Subsequently, a blend film of PSBTBT/$PC_{71}BM$ was spincoated and a PVA film of 50 nm was spincoated again on the blend film. Finally a semi-transparent metal electrode of Au (15 nm) was thermally deposited under vacuum at 4×10^{-4} Pa and the device was encapsulated with a glass cover in a nitrogen-protected glove box. The device was excited with a pulse laser at 532 nm and probed at 1200 nm. Detailed information of transient absorption measurements has been described elsewhere[19,20]. To generate electric field across the active layer, a square pulse voltage that covers the time range of

measurements was applied to the device with a function generator (NF, WF1973). The voltage was applied for 20 μs from 5 μs before the excitation.

3. Results and discussion

3.1 TPV/TPC analysis

Figure 2 shows the *J*–*V* curve of a PSBTBT/$PC_{71}BM$ solar cell. The short-circuit current density (J_{SC}) was 11.9 mA cm^{-2}, the open-circuit voltage (V_{OC}) was 0.55 V, the FF was 0.46, and the PCE was 3.0%. The V_{OC} and the FF were lower than those reported previously[18,21,22], probably because the active layer (180 nm) was thicker than optimal value. As shown in the figure, the photocurrent was clearly voltage-dependent even at around the short-circuit, suggesting that charge generation and/or collection are dependent upon voltage. As a result, the FF was as low as less than 0.5. For this photovoltaic device, TPV/TPC measurements were performed.

In TPV measurements, minority charges are generated by a small perturbation light from the pulse laser, and they recombine with major charges generated by bias illumination. Under these conditions, the recombination can be treated as pseudo-first-order reaction, and therefore the transient voltage decay is given by a single exponential Eq. (1)[23]

$$\Delta V = \Delta V_0 \exp\left(-\frac{t}{\tau_{\Delta n}}\right) \quad (1)$$

where ΔV_0 is the initial photovoltage increment and $\tau_{\Delta n}$ is the lifetime of minority charges under the bias illumination. Figure 3 shows the semi-logarithmic plots of the $\tau_{\Delta n}$ against V_{OC} under different bias illumination intensities. As shown in the figure, the lifetime of minority charges is given by a single exponential Eq. (2)

$$\tau_{\Delta n} = \tau_{\Delta n_0} \exp\left(-\frac{qV_{OC}}{\nu k_B T}\right) \quad (2)$$

where $\tau_{\Delta n_0}$ is the extrapolated lifetime at V_{OC} = 0, q is the elementary charge, k_B is the Boltzmann constant, T is the absolute temperature, and ν is the ideality factor of charge carrier lifetime. From the slope in the figure, ν was evaluated to be 2.1.

In TPC measurements, the amount of charges generated by the pulse laser Δq is obtained from the integral of the transient photocurrent over the time. The differential capacitance dC is defined by Eq. (3)

$$dC(V_{OC}) = \frac{\Delta q}{\Delta V_0(V_{OC})} \quad (3)$$

where $\Delta V_0(V_{OC})$ is the initial photovoltage increment obtained by Eq. (1). As a result, the charge density n is given by Eq. (4)

$$n = \frac{1}{qAL}\int_0^{V_{OC}} \mathrm{d}C(V_{OC})\mathrm{d}V \quad (4)$$

where L is the thickness and A is the area of the device. Figure 4 shows the plots of n against V_{OC} under different bias illumination intensities. As shown in the figure, the charge density is given by a single exponential Eq. (5)

$$n = n_0 \exp\left(\frac{qV_{OC}}{mk_BT}\right) \quad (5)$$

where n_0 is the extrapolated charge density at $V_{OC} = 0$ and m is the ideality factor of charge density. From the slope in the figure, m was evaluated to be 4.5. By using these parameters obtained, overall charge lifetime τ_n is given by Eq. (6)

$$\tau_n = (\nu/m + 1)\tau_{\Delta n} = (\lambda + 1)\tau_{\Delta n} \quad (6)$$

where $\lambda + 1$ represents reaction order of recombination[23]. Here, $\lambda + 1$ was evaluated to be 3.2. Figure 5 shows the log-log plots of τ_n against n. Under 1 sun illumination, the charge lifetime τ_n was evaluated to be 4.1 μs and the charge density n to be 3.3×10^{16} cm^{-3}. Using these values, the bimolecular recombination rate constant is obtained by Eq. (7)

$$k_{rec} = \frac{1}{\tau_n n} \quad (7)$$

On the other hand, the diffusion-limited Langevin recombination rate constant is given by Eq. (8)[24]

$$k_L = \frac{q\mu}{\varepsilon\varepsilon_0} \quad (8)$$

where μ is the slower charge mobility[25], ε is the dielectric constant, and ε_0 is the vacuum permittivity. Here, the dielectric constant is assumed to be 3.5 for PSBTBT/$PC_{71}BM$ blend films. The hole mobility listed in Table I was evaluated for hole-only device (ITO/PEDOT:PSS/PSBTBT:$PC_{71}BM$/Au) by the space-charge-limited current (SCLC) method. The recombination reduction factor is defined by $\zeta = k_{rec}/k_L$. As shown in the Table II, ζ of the PSBTBT/$PC_{71}BM$ solar cell is of the order of 10^{-2}, which is comparable to that of PNTz4TF*x*/PCBM solar cells[13]. In other words, the bimolecular recombination in PSBTBT/$PC_{71}BM$ solar cells is equally suppressed as in PNTz4TF*x*/$PC_{71}BM$ solar cells under open-circuit condition.

3.2 *J–V* analysis

Using recombination parameters obtained by TPV/TPC measurements, experimental *J*–*V* curves can be analyzed. Current density under illumination is expressed by Eq. (9)[27,28]

$$J(V) = J_{\mathrm{GEN}}(V) + J_{\mathrm{BR}}(V) \tag{9}$$

where J_{GEN} is charge generation current density and J_{BR} is bimolecular recombination current density. Here, J_{GEN} is assumed to be constant, which is evaluated as saturated current density J_{sat} at −2 V. On the other hand, J_{BR} is given by Eq. (10)

$$J_{\mathrm{BR}} = -\frac{qLn(V)}{\tau_n} \tag{10}$$

By using a power law equation $\tau_n = \tau_0 n^{-\lambda}$, J_{BR} is expressed as Eq. (11)

$$J_{\mathrm{BR}} = -\frac{qLn(V)^{\lambda+1}}{\tau_0} \tag{11}$$

The voltage-dependent charge density $n(V)$ was estimated as follows. The charge density at open circuit was evaluated by the TPV/TPC measurements. On the other hand, the charge density at short circuit is estimated by Eqs. (12) and (13) with a charge collection time τ_{CC}

$$n_{\mathrm{SC}} = \frac{J_{\mathrm{SC}}\tau_{\mathrm{CC}}}{qL} \tag{12}$$

$$\tau_{\mathrm{CC}} = \frac{L^2}{2\mu V_{\mathrm{b}}} \tag{13}$$

where V_{b} is the built-in potential that is assumed to be V_{OC} at short circuit. As reported previously,[29] charge density typically increases exponentially with increasing voltage. Here, we therefore assumed that $n(V)$ is given by an exponential function. Thus, *J*–*V* curves can be estimated by using the following two parameters: $n(0) = n_{\mathrm{SC}}$ and $n(V_{\mathrm{OC}}) = n_{\mathrm{OC}}$.[13] As shown in Figure 2, the *J*–*V* curve estimated largely deviates from that obtained experimentally. The photocurrent is overestimated, especially at around short-circuit condition. This disagreement suggests that the two conditions we assumed would be not correct: one is that J_{GEN} is assumed to be constant independently of bias voltage and the other is that $n(V)$ is given by an exponential function with $n(0) = n_{\mathrm{SC}}$ and $n(V_{\mathrm{OC}}) = n_{\mathrm{OC}}$. In order to address the origin of this disagreement, we reconsider the two assumptions as mentioned below.

3.3 Charge generation

First, we consider the voltage dependence of J_{GEN} in PSBTBT/$PC_{71}BM$ solar cells. We thus measured transient absorption of PSBTBT/$PC_{71}BM$ blend films under bias voltages.

Figure 6 shows the transient absorption decay of polymer polarons generated in the blend film excited at 532 nm under different applied voltages. The effective voltage V_{eff} applied across the blend film is estimated by considering the PVA interlayers with an assumed dielectric constant of 2[30]. As shown in the figure, no transient decay was observed at an early time stage of <0.3 μs, indicating negligible bimolecular recombination. We therefore estimate the amount of charge carriers generated from the initial transient signals. Figure 7 shows the plots of initial transient signal amplitude against effective applied voltages. Here, effective voltage corresponds to the built-in voltage for solar cells under operating condition. The initial amplitude is only weakly voltage dependent over the effective voltage range from 0 to 1 V, which corresponds to $-0.5\ \mathrm{V} < V < 0.5\ \mathrm{V}$ range in Fig. 2. This finding shows that the photocurrent generation can be assumed to be independent of applied voltages. In other words, the first condition we assumed is valid in PSBTBT/PC_{71}BM solar cells.

3.4. Bimolecular recombination

Next, we consider the second assumption that $n(V)$ is given by an exponential function with $n(0) = n_{SC}$ and $n(V_{OC}) = n_{OC}$. As mentioned above, n_{OC} was evaluated experimentally by TPV/TPC measurements. On the other hand, n_{SC} was estimated by Eqs. (12) and (13) with a hole mobility measured for the hole-only device. As shown in Table 1, the hole mobility of PSBTBT/PCBM is as low as a quarter of the electron mobility. Such imbalanced mobilities would cause charge accumulation in the active layer, which screens the built-in electric field, as reported previously[31,32]. A numerical simulation study has shown that the charge density at short circuit would increase by almost an order of magnitude under the imbalanced charge mobilities with an order of magnitude difference[33]. In addition, the hole mobility of PSBTBT/PC_{71}BM is one order of magnitude lower than that of PNTz4T/PC_{71}BM. A recent study has shown that low mobilities cause charge accumulation and increase bimolecular recombination even if they are balanced[34]. We therefore speculate that n_{SC} would be higher than that we assumed before and hence bimolecular recombination is still dominant even under the short-circuit condition. If we assume that n_{SC} is as high as $2.3 \times 10^{16}\ \mathrm{cm^{-3}}$, which is about 6 times larger than that we estimated, J_{BR} is estimated to be 6.1 mA $\mathrm{cm^{-2}}$ at short circuit. We therefore conclude that

the low FF of the PSBTBT/$PC_{71}BM$ solar cell originates from the bimolecular recombination under the short-circuit condition even though bimolecular recombination is intrinsically well suppressed under the open-circuit condition as is the case with PNTz4TF*x*/$PC_{71}BM$ solar cells. This is due to the charge accumulation caused by low and imbalanced mobilities.

4. Conclusions

We studied charge recombination losses in a PSBTBT/$PC_{71}BM$ solar cell by measuring transient optoelectronic techniques. Based on transient absorption measurements, photocurrent generation was almost voltage-independent, indicating that FF is not largely affected by geminate recombination. On the other hand, based on transient photovoltage/transient photocurrent measurements, bimolecular recombination under open-circuit condition was suppressed by two orders of magnitude compared to diffusion-limited Langevin recombination. We also found that the hole mobility is relatively low and a quarter of the electron mobility by SCLC method. Such low and imbalanced mobilities can cause the accumulation of charges and accelerate bimolecular recombination. We thus concluded that the low FF of the solar cell originates from inefficient charge collection because of the charge accumulation. We therefore conclude that not only reduced bimolecular recombination at open circuit but also efficient charge collection at short circuit are required for high FF with a thick active layer.

Acknowledgments

This work was supported by the JST Advanced Low Carbon Technology Research and Development (ALCA) program (Solar Cell and Solar Energy Systems).

References

1) M. A. Green, Y. Hishikawa, W. Warta, E. D. Dunlop, D. H. Levi, J. Hohl-Ebinger, and A. W. Y. Ho-Baillie, Prog. Photovolt. Res. Appl. **25**, 668 (2017).
2) S. H. Liao, H. J. Jhuo, P. N. Yeh, Y. S. Cheng, Y. L. Li, Y. H. Lee, S. Sharma, and S. A. Chen, Sci. Rep. **4**, 6813 (2014).
3) Y. Liu, J. Zhao, Z. Li, C. Mu, W. Ma, H. Hu., K. Jiang, H. Lin, H. Ade, and H. Yan, Nat. Commun. **5**, 5293 (2014).
4) V. Vohra, K. Kawashima, T. Kakara, T. Koganezawa, I. Osaka, K. Takimiya, and H. Murata, Nat. Photon. **9**, 403 (2015).
5) W. Zhao, S. Li, H. Yao, S. Zhang, Y. Zhang, B. Yang, and J. Hou, J. Am. Chem. Soc. **139**, 7148 (2017).
6) S. Albrecht, S. Schäfer, I. Lange, S. Yilmaz, I. Dumsch, S. Allard, U. Scherf, A. Hertwig, and D. Neher, Org. Electron. **13**, 615 (2012).
7) S. H. Park, A. Roy, S. Beaupré, S. Cho, N. Coates, J. S. Moon, D. Moses, M. Leclerc, K. Lee, and A. J. Heeger, Nat. Photon. **3**, 297 (2009).
8) Y. Liang, Z. Xu, J. Xia, S. T. Tsai, Y. Wu, G. Li, C. Ray, and L. Yu, Adv. Mater. **22**, E135 (2010).
9) G. Li, V. Shrotriya, J. Huang, Y. Yao, T. Moriarty, K. Emery, and Y. Yang, Nat. Mater. **4**, 864 (2005).
10) H. Choi, S. J. Ko, T. Kim, P. O. Morin, B. Walker, B. H. Lee, M. Leclerc, Jin. Young Kim, and A. J. Heeger, Adv. Mater. **27**, 3318 (2015).
11) S. C. Price, A. C. Stuart, L. Yang, H. Zhou, and W. You, J. Am. Chem. Soc. **133**, 4625 (2011).
12) K. Kawashima, I. Osaka, and K. Takimiya, Chem. Mater. **27**, 6558 (2015).
13) K. Kawashima, T. Fukuhara, Y. Suda, Y. Suzuki, T. Koganezawa, H. Yoshida, H. Ohkita, I. Osaka, and K. Takimiya, J. Am. Chem. Soc, **138**, 10265 (2016).
14) Y. Tamai, K. Tsuda, H. Ohkita, H. Benten, and S. Ito, Phys. Chem. Chem. Phys, **16**, 20338 (2014).
15) H. Lv, X. Zhao, W. Xu, H. Li, J. Chen, and X. Yang, Org. Electron. **14**, 1874 (2013).
16) J. Hou, H. Y. Chen, S. Zhang, G. Li, and Y. Yang, J. Am. Chem. Soc. **130**, 16144 (2008).
17) H. Y. Chen, J. Hou, A. E. Hayden, H. Yang, K. N. Houk, and Y. Yang, Adv. Mater. **22**, 371

(2010).

18) J. Peet, L. Wen, P. Byrne, S. Rodman, K. Forberich, Y. Shao, N. Drolet, R. Gaudiana, G. Dennler, and D. Walker, Appl. Phys. Lett. **98**, 043301 (2011).
19) H. Ohkita, Y. Tamai, H. Benten, and S. Ito, IEEE J. Sel. Top. Quantum. Electron. **22**, 4100612 (2016).
20) Y. Kasai, Y. Tamai, H. Ohkita, H. Benten, and S. Ito, J. Am. Chem. Soc. **137**, 15980 (2015).
21) F. Etzold, I. A. Howard, N. Forler, A. Melnyk, D. Andrienko, M. R. Hansen, and F. Laquai, Energy Environ. Sci. **8**, 1511 (2015).
22) A. Colsmann, A. Puetz, A. Bauer, J. Hanisch, E. Ahlswede, and U. Lemmer, Adv. Energy Mater. **1**, 599 (2011).
23) A. Maurano, C. G. Shuttle, R. Hamilton, A. M. Ballantyne, J. Nelson, W. Zhang, M. Heeney, and J. R. Durrant, J. Phys. Chem. C **115**, 5947 (2011).
24) B. P. Rand and H. Richter, *Organic Solar Cells: fundamentals, devices, and upscaling* (CRC Press, Boca Raton, FL, 2014) p. 439.
25) L. J. A. Koster, V. D. Mihailetchi, and P. W. M. Blom, Appl. Phys. Lett. **88**, 052104 (2006).
26) K. R. Choudhury, J. Subbiah, S. Chen, P. M. Beaujuge, C. M. Amb, J. R. Reynolds, and F. So, Sol. Energ. Mater. Sol. Cells **95**, 2502 (2011)
27) D. Credgington and J. R. Durrant, J. Phys. Chem. Lett. **3**, 1465 (2012).
28) D. Credgington, F. C. Jamieson, B. Walker, T.Q. Nguyen, and J. R. Durrant, Adv. Mater. **24**, 2135 (2012).
29) G. F. A. Dibb, F. C. Jamieson, A. Maurano, J. Nelson, and J. R. Durrant, J. Phys. Chem. Lett. **4**, 803 (2013).
30) T. A. Hanafy, J. Appl. Polym. Sci. **108**, 2540 (2008).
31) V. D. Mihailtchi, J. Wildeman, and P. W. M. Blom, Phys. Rev. Lett. **94**, 126602 (2005).
32) J. D. Kotlarski, D. J. D. Moet, and P. W. M. Blom, J. Polym. Sci. Part B: Polym. Phys. **49**, 708 (2011).
33) J. T. Shieh, C. H. Liu, H. F. Meng, S. R. Tseng, Y. C. Chao, and S. F. Horng, J. Appl. Phys. **107**, 084503 (2010).
34) J. A. Bartelt, D. Lam, T. M. Burke, S. M. Sweetnam, and M. D. McGehee, Adv. Energy Mater. **5**, 1500577 (2015).

Figure Captions

Fig. 1. (black and white) Chemical structures of materials: a) PSBTBT and b) $PC_{71}BM$.

Fig. 2. (black and white) *J*–*V* curves of the solar cell measured (open circles) and calculated (solid line) by Eq. (9) with the recombination parameters obtained by TPV/TPC measurements.

Fig. 3. (black and white) Semi-logarithmic plots of the lifetimes of charges generated by pulse laser in the solar cell against open-circuit voltage under different bias illumination intensities. The solid lines represent a fitting line by Eq. (2).

Fig. 4. (black and white) Semi-logarithmic plots of the charge densities in the solar cell against open-circuit voltage under different bias illumination intensities. The solid line represents a fitting line by Eq. (5).

Fig. 5. (black and white) Log-log plots of the overall lifetimes of charges in the solar cell against the charge densities.

Fig. 6. (black and white) Transient absorption decay at 1200 nm of a PSBTBT/$PC_{71}BM$ blend film excited at 532 nm with a fluence of 1.8 μJ cm^{-2} under effective applied voltage of 0, 0.53, 1.05, and 1.58 V. The solid lines represent the fitting curves by a power-law function: $\Delta OD(t) = \Delta OD_0/(1 + at)^{\alpha}$.

Fig. 7. (black and white) Voltage dependence of the initial signal of the transient decay ΔOD_0.

Table I. Charge mobility in each blend film.

Blends	μ_h / cm^2 V^{-1} s^{-1}	μ_e / cm^2 V^{-1} s^{-1}
PNTz4T/PC$_{71}$BM[13)]	3.4×10^{-3}	1.1×10^{-3}
PNTz4TF2/PC$_{71}$BM[13)]	1.5×10^{-3}	2.1×10^{-3}
PSBTBT/PC$_{71}$BM	3.3×10^{-4}	1.2×10^{-3} [26)]

Table II. Kinetic parameters for bimolecular recombination in polymer solar cells.

Blends	k_{rec} / cm^3 s^{-1}	k_L / cm^3 s^{-1}	ζ	FF
PNTz4T/PC$_{71}$BM[13)]	7.5×10^{-12}	5.8×10^{-10}	0.01	0.72
PNTz4TF2/PC$_{71}$BM[13)]	2.1×10^{-11}	7.9×10^{-10}	0.03	0.65
PSBTBT/PC$_{71}$BM	6.1×10^{-12}	1.7×10^{-10}	0.04	0.46

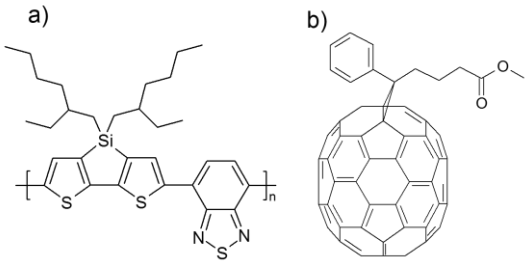

Fig. 1. (black and white)

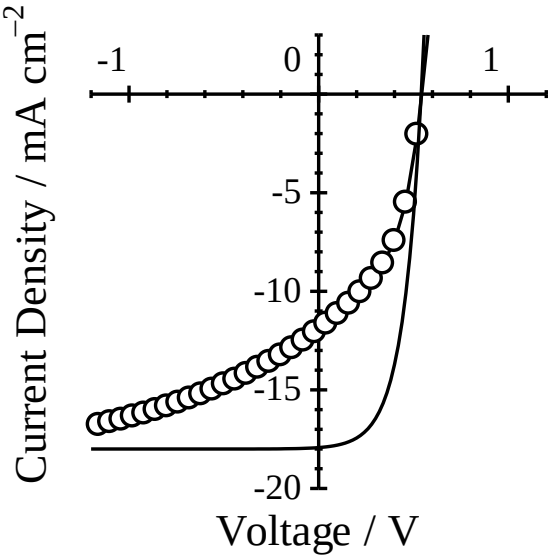

Fig. 2. (black and white)

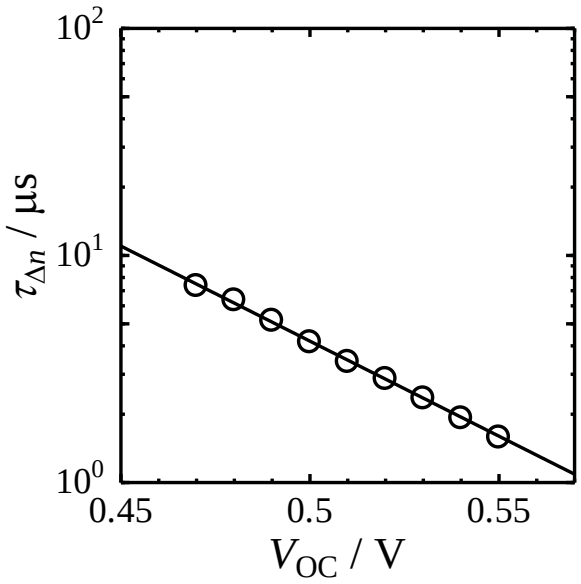

Fig. 3. (black and white)

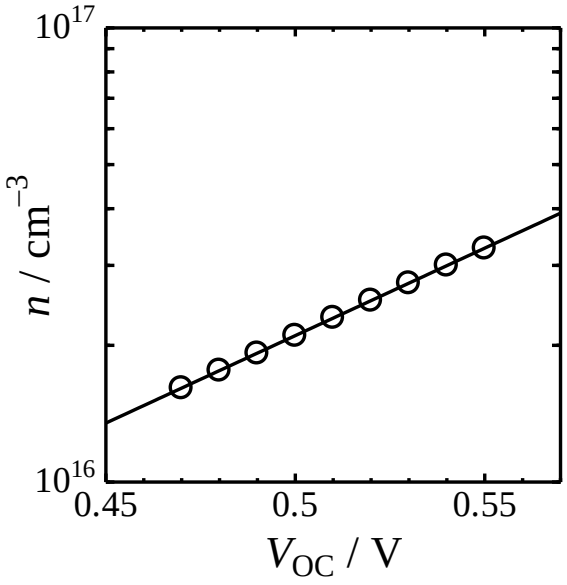

Fig. 4. (black and white)

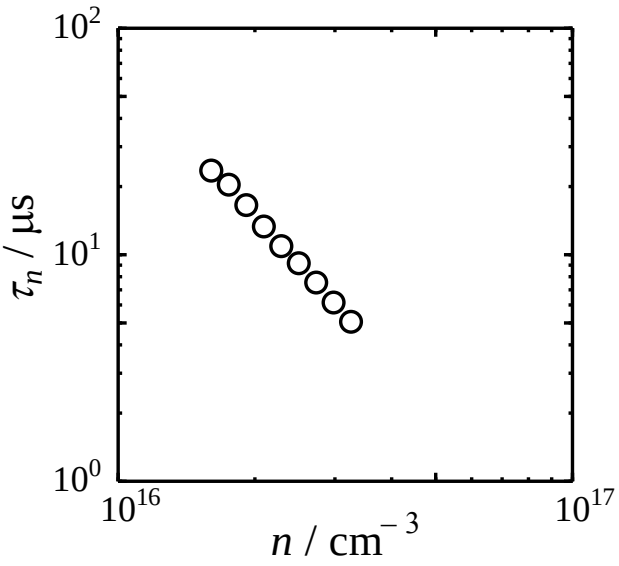

Fig. 5. (black and white)

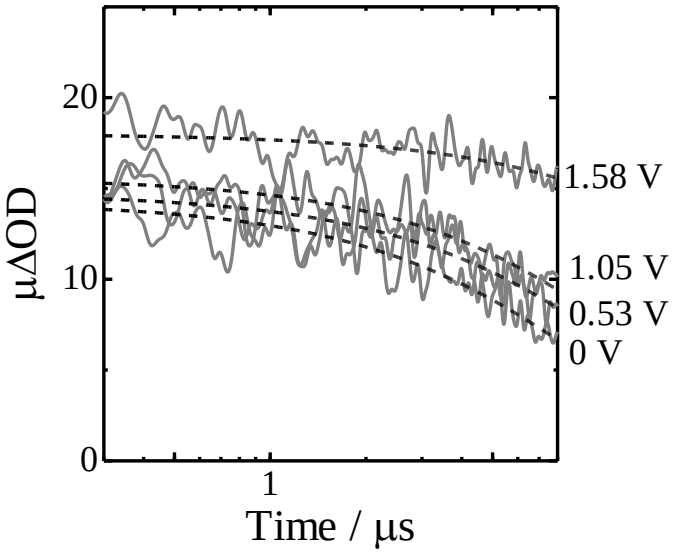

Fig. 6. (black and white)

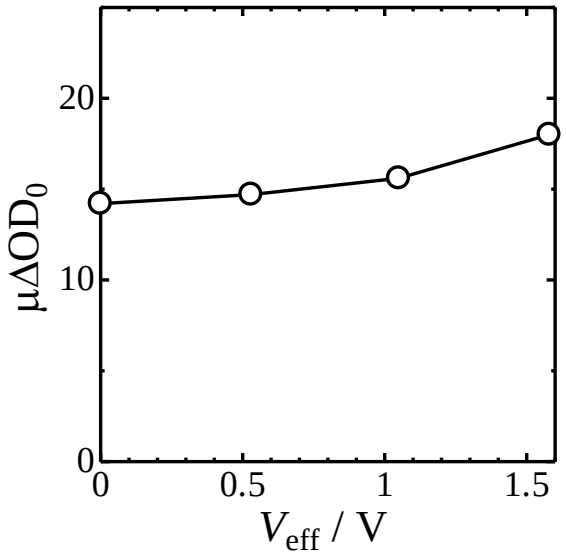

Fig. 7. (black and white)